ORAL/POSTER REFERENCE: ICF10023OR

MICROMECHANISMS OF FATIGUE IN POLYSILICON MEMS STRUCTURES

S. M. Allameh[+], P. Shrotriya[+], B. Gally[x], S. Brown[x] and W.O. Soboyejo[+]

[+]The Princeton Materials Institute and Department of Mechanical and Aerospace Engineering, Princeton University, 1 Olden Street, Princeton, NJ 08544
[x]Exponent Failure Analysis and Associates, 21 Strathmore Road, Natick, MA 01760

ABSTRACT

This paper presents the results of a combined experimental and computational study of crack nucleation and surface topology evolution during the cyclic actuation of polysilicon MEMS structures. The evolution in surface topology observed during the crack nucleation stage is related to the underlying notch-tip stress distributions calculated using finite element analysis. Measured changes in surface topology due to the stress-assisted dissolution of silica are shown to be predicted by linear stability analysis.

KEYWORDS

Polysilicon MEMS, fatigue, surface reaction, stress-assisted dissolution, surface topology evolution, linear stability analysis

INTRODUCTION

Micro-Electro-Mechanical Systems (MEMS) fabricated from polysilicon are extensively used in a wide range of applications in which fatigue failure is possible [1-9]. These include applications ranging from accelerometers, actuators and pressure sensors [1,2], in which cyclic loads can ultimately lead to the nucleation and propagation of cracks. Unfortunately, however, the current understanding of fatigue in polysilicon is still limited.

The initial work on the fatigue of silicon MEMS structures was done by Brown and co-workers [3-5]. They obtained stress-life and fatigue crack growth rate data that suggested a strong influence of water vapor on the fatigue of polysilicon. More recently, Kahn et al. [6], Muhlstein et al. [7], Sharpe et al. [8] and Allameh et al. [9] have also reported the result of experimental studies of fatigue in polysilicon. Most of these studies have suggested that the overall fatigue life in polysilicon MEMS is dominated by the crack nucleation stage [3-9].

The paper presents the results of a combined experimental and computational/analytical study of the possible role of surface topology evolution in the nucleation of fatigue cracks in notched polysilicon MEMS structures.

Evidence of surface topology evolution obtained from atomic force microscopy is analyzed using Fourier analysis techniques. Evidence of surface topology evolution is presented along with finite element analysis of the notch-tip stress distributions that suggest a strong influence of stress state on the topology evolution. The measured surface topologies obtained using atomic force microscopy (AFM) are also compared with predictions from linear perturbation analysis of the stability of surface topology that evolves during stress-assisted dissolution of the silica layer that is present due to the surface oxidation of Si.

MATERIAL

The polysilicon MEMS structures that were used in this study were supplied by Cronos Integrated Microsystems (formerly MCNC) of Raleigh-Durham, NC. The MEMS structures were fabricated in batch runs at Cronos. Details of the micromachining processing schemes are given in Ref. [2]. The polysilicon MEMS structures consist of a capacitive comb-drive attached to the end of a notched sample as shown in Fig.1 (a). The devices were sealed under a topical SiO_2 layer that was removed before actuation. The release process consisted of rinsing in acetone, dissolving topical SiO_2 in concentrated (49.6%) hydrofluoric acid, rinsing in distilled water, followed by rinsing in propanol and drying in air at 110^{o}C. The surface of the structures was studied initially in a scanning electron microscope (SEM) to examine the microstructure, grain size and porosity. A secondary electron image of the polysilicon is presented in Fig. 1(b). This shows an equiaxed microstructure consisting of nano-size grains, with an average grain size of ~200 nm, and distributed porosity at the triple points.

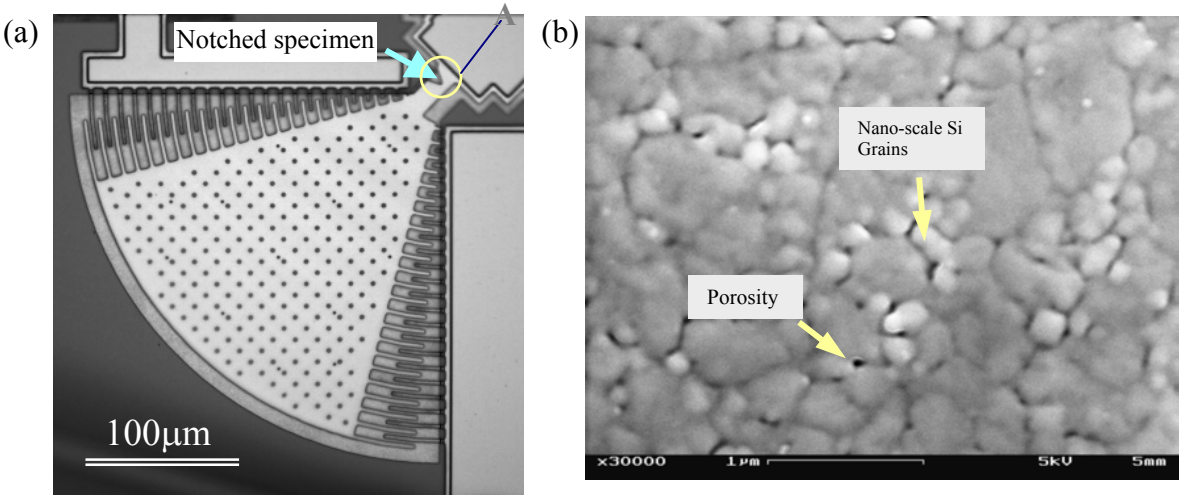

Figure 1 Notched polysilicon sample: (a) Photograph of a notched comb drive structure, (b) Scanning electron micrograph of polysilicon MEMS structure before actuation.

EXPERIMENTAL PROCEDURE

Atomic force microscopy (AFM) was used to characterize the surface morphology of the polysilicon sample before, during, and after cyclic actuation. The characterization included scanning of the specimen surface (labeled A in Fig. 1) immediately below the bottom of the notch where tensile stresses are highest during actuation. Two scan sizes (2µm x 2µm and 5µm x 5µm) were chosen to study both the extent and magnitude of the superficial morphological changes that occur during cyclic actuation. Following specimen calibration using techniques described by Van Arsdell et al. [5], the polysilicon structures were actuated at a constant actuation

voltage of 145 V through the application of an alternating direct current that was generated from a programmable wave function generator and amplified. The angular displacements of the actuating structures were examined using an optical microscope that was connected to a video recorder, and a microvision system [10]. AFM images were obtained during the cyclic actuation of the polysilicon MEMS structures. These were used to measure the morphological changes in the areas of highest tensile stress in the vicinity of the notches. The measured changes in surface topology were then analyzed using Fourier analysis techniques [11,12].

Polysilicon structures tested in this study show significant surface changes that occur after cyclic actuations for 2×10^9 cycles with a constant angular displacement of 1.44 degrees. AFM images obtained from the area at the bottom of the notch before and after actuation are presented in Fig. 2. There is a significant change in the surface topology before actuation (Fig. 2a) and after actuation (Fig. 2b) in an area of 5 μm x 5 μm. The observed changes in the surface topology may be ascribed to a stress assisted dissolution of SiO_2 that can give rise to the evolution of grooves and ultimately to the nucleation of fatigue cracks [11,12].

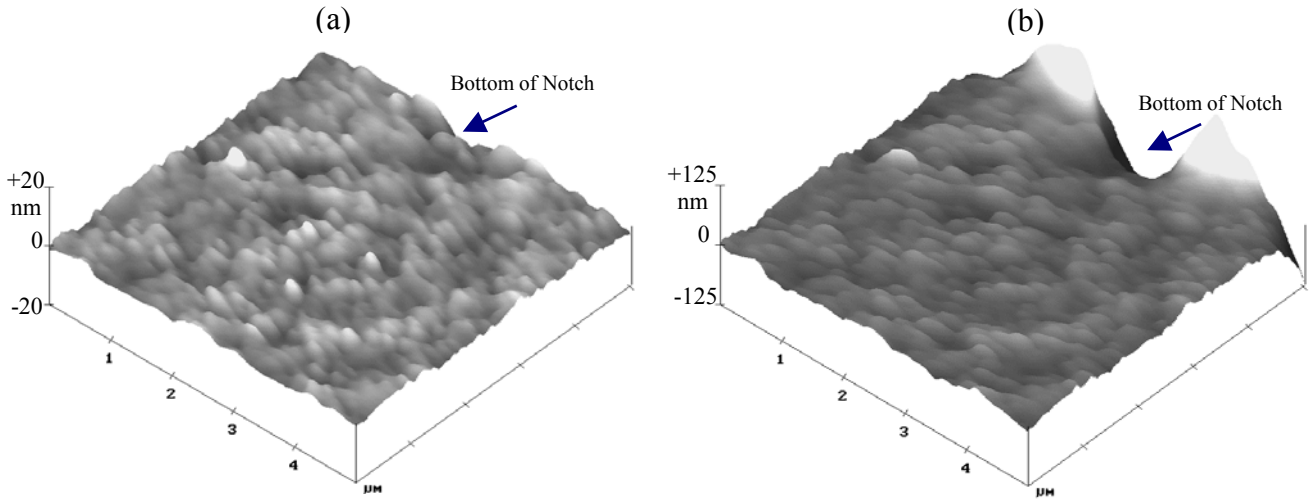

Figure 2 AFM images showing surface evolution of the silicon MEMS sample under cyclic loading conditions. (a) Before actuation and (b) after actuation.

MODELING

Finite element Analysis

The stress distribution at notch-tip corresponding to the measured angular displacement was modeled using finite-element analysis in order to determine the relationship between the observed angular displacement and maximum principal stress, σ_{max}. The geometry of the notch was determined from the measured values, while the dimensions of the specimen were taken from the nominal design. The model was constructed from the 6,200 six-noded plane stress triangular elements. The mesh density was determined by a study of the numerical convergence of stress distribution with the number of elements. For the analysis, Young's modulus and Poisson's ratio of polysilicon were assumed to be 147 GPa and 0.22, respectively and a linear elastic small strain formulation was used. The finite element analysis was performed using ABAQUS. The typical results of the finite element analysis are presented in Fig. 3. Figure 3(a) shows the details of the discretization near the notch-tip and Fig. 3(b) shows the contour of maximum principal stress in the region surrounding the notch-tip corresponding to an angular displacement of 1.44°.

Linear Perturbation Analysis

Kim et al. [11] and Yu and Suo [12] have used linear perturbation analysis to study the dissolution of a stressed solid surface and related the change in surface profile to the stress state. A similar analysis is utilized here to study the observed roughening of the SiO_2 layer on the polysilicon MEMS structures. Following Yu and Suo [12], a linear perturbation analysis is utilized in order to correlate the time evolution of individual Fourier components of the surface roughness to applied stress state. The perturbation analysis is performed by assuming that the surface mobility is independent of the stress state [11, 12]. The time evolution of the amplitude of a Fourier component, $q(\omega,t)$, at an angle θ to the principal axes, *is* expressed as [11, 12]:

$$\ln\frac{q(\omega,t)}{q(\omega,0)} = M\alpha t\,. \tag{1}$$

Where M is the surface mobility associated with the dissolution reaction, t is the time and α is given by [11,12]:

$$\alpha = \frac{2(1+\nu)}{E}\left[(1-\nu)\left(\sigma_1\cos^2\theta + \sigma_2\sin^2\theta\right)^2 + (\sigma_1-\sigma_2)^2\cos^2\theta\sin^2\theta\right]\omega - \gamma\omega^2\,. \tag{2}$$

E is the Young's modulus, ν is the Poisson's ratio, γ is the surface energy per unit area and σ_1 and σ_2 are the in-plane principal stresses.

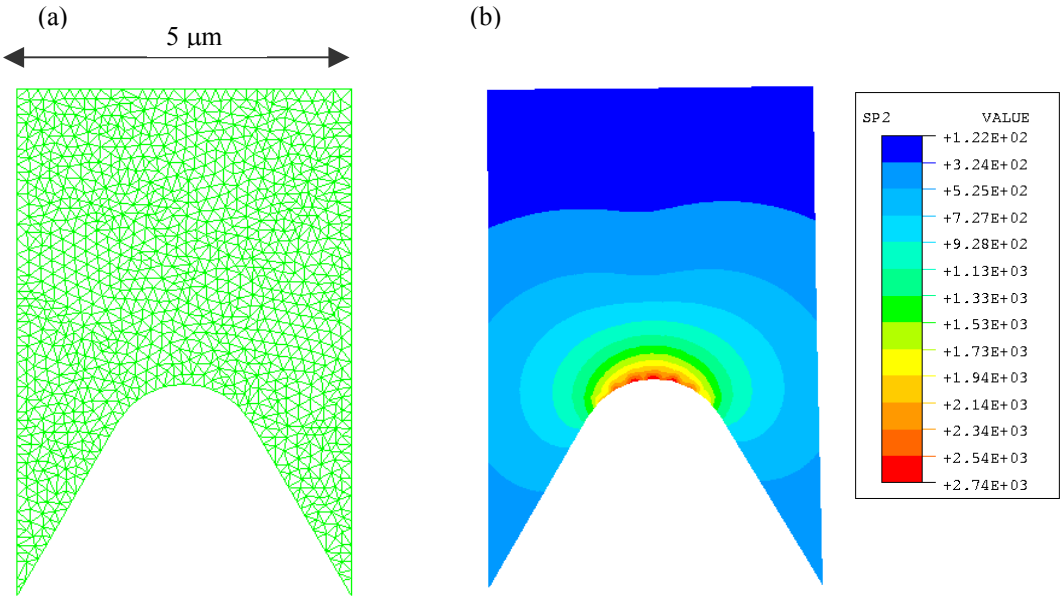

Figure 3 Finite element calculations: (a) Details of the discretization near the notch-tip, (b) Principal stress distribution near the notch-tip corresponding to angular displacement of 1.44°.

The quantity, α, corresponding to stress state at base of the notch, is evaluated for the different Fourier components in order to study the influence of the stress-assisted surface reaction. During the experiments, the MEMS structure was loaded under cyclic loading hence the root mean square (RMS) average of principal stresses is utilized in the calculations. The RMS average of the in-plane stresses at the base of the notch are

computed to be σ_{11} = 1990 MPa, σ_{22} = 141 MPa and σ_{12} = 0. The interfacial energy of the SiO_2 and water system is reported equal to 4.8 Jm^{-2} (46 ergs cm^{-2}) [13]. The contour plot of α corresponding to the stress state is presented in Fig. 4. The dark thick contour line on the plots corresponds to $\alpha = 0$ and α is positive for all the wave numbers enclosed by it.

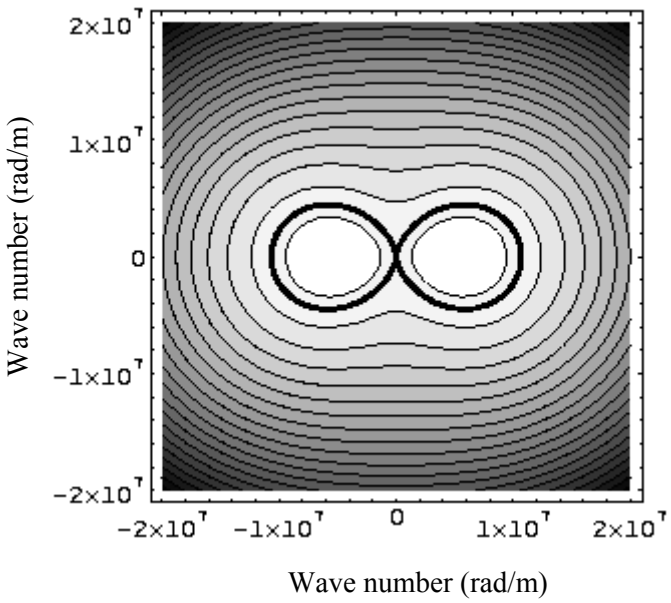

Figure 4 Contours of a corresponding to the stress state at the notch-tip

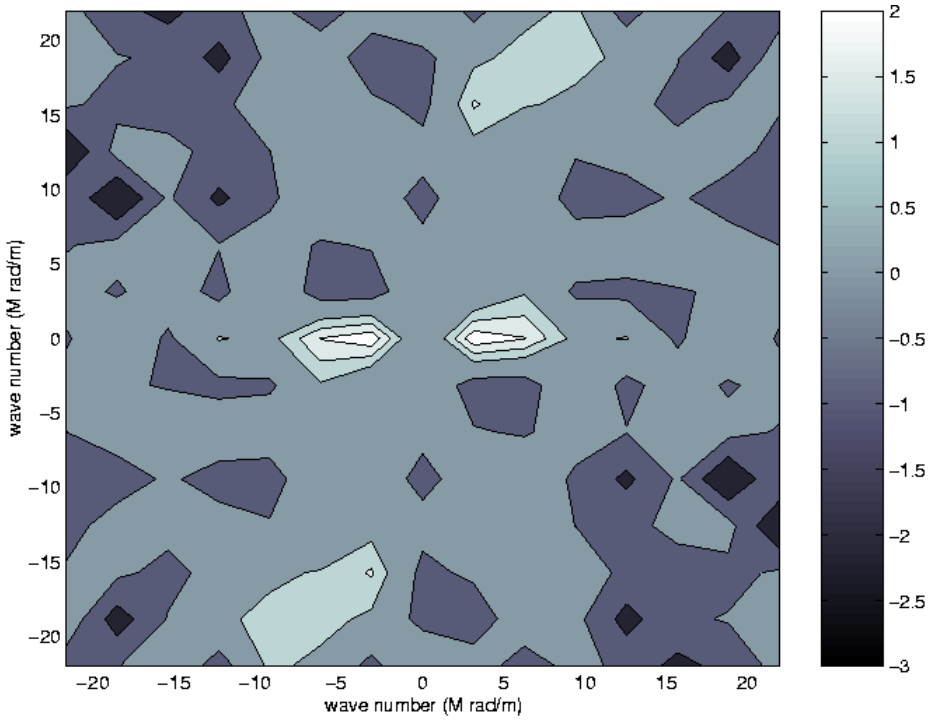

Figure 5 Contours of $\ln q(\omega,t)/q(\omega,0)$ corresponding to an area of 2 μm x 2 μm near the notch-tip.

Following the procedure described by Kim et al. [11], the quantity on the left hand side of Eq. (1) was evaluated using the measured surface morphologies of the MEMS structure before and after the cyclic actuation. The contours of $\ln q(\omega,t)/q(\omega,0)$ corresponding to the areas of 2μm x 2μm area, near the notch-tip are plotted in Fig. 5. Comparison of the contour plots of $\ln q(\omega,t)/q(\omega,0)$ and α indicates that the shape of the contours is similar. Additionally, the magnitude of the wave numbers predicted to grow by linear perturbation analysis compare remarkably well with the experimental measurements.

SUMMARY AND CONCLUDING REMARKS

1. AFM images obtained from 2x2μm and 5x5μm of the area located on the surface of the structure at the bottom of the notch show that significant changes in surface topology occur in polysilicon during cyclic actuation.
2. The finite element analysis shows that the highest principal stress levels occur in the regions where the evolution of surface topology results in formation of deep grooves.
3. Time evolution of the surface roughness indicates that amplitudes of a few wave numbers grow with time during cyclic actuation. This effect may be attributed to stress-assisted interactions between water molecules and the SiO_2 layer on the surfaces of the notched specimens in the regions at the bottom of the notch.

ACKNOWLEDGEMENTS

The research was supported by the Division of Materials Research of The National Science Foundation (NSF) and The Defense Arms Research Projects Agency (DARPA). WOS, PS and SA are grateful to Dr. Jorn Larsen-Basse, the program manager at NSF, for his encouragement and support. Appreciation is also extended to Alex Butterwick and Hadi Allameh for assistance with experimental techniques.

REFERENCES

1. K.D. Wise and K. Najafi (1991) *Science*, 254, 1335.
2. M. Madou (1997) *Fundamentals of Microfabrication*, CRC Press, New York.
3. J.A. Connally and S.B. Brown (1992) *Science*, 256, 1537.
4. J.A. Connally and S.B. Brown (1993) *Experimental Mechanics*, 33, 81.
5. W. Van Arsdell and S. Brown (1999) *J. Microelectromech. Syst.,* 46, 320.
6. H. Kahn, R. Ballarini, R. L. Mullen and A. H. Heuer (1990) *Proc. Roy. Soc., Series A* 455, 3807.
7. C. Muhlstein, S. Brown and R. O. Ritchie (2001) In: *Mechanical properties of structural films,* STP 1413, C. Muhlstein and S. Brown (Eds). American society for testing and materials, West Conshohocken. (in press).
8. W. N. Sharpe Jr., B. Yuan and R. L. Edwards (1999). In: *Proc. Fatigue'99*, pp. 1837-1844.
9. Allameh, S. M. Gally, B. Brown, and W. O. Soboyejo (2001). In: *Mechanical properties of structural films,* STP 1413, C. Muhlstein and S. Brown (Eds). American society for testing and materials, West Conshohocken. (in press)
10. D. M. Freeman, A. J. Aranyosi, M. J. Gordon (1998), In: *Proc. Solid-State Sensor and Actuator Workshop, Hilton Head Island, SC*. 150-155.
11. K. S. Kim, J. A. Hurtado and H. Tan (1999) *Phys Rev. Lett.*, 83, 3872.
12. H. H. Yu and Z. Suo (2000) *J. Appl. Phys.*, 87, 1211.
13. R. K. Iler (1979). *Chemistry of Silica*, John Wiley & Sons, New York.